Preferential interaction between DNA and small ions in mixed-size counterion systems: Monte Carlo simulation and density functional study

Ke Wang, Yang-Xin Yu,[a] Guang-Hua Gao, and Guang-Sheng Luo
Department of Chemical Engineering, Tsinghua University, Beijing 100084, People's Republic of China and State Key Laboratory of Chemical Engineering, Tsinghua University, Beijing 100084, People's Republic of China

(Received 27 December 2006; accepted 8 February 2007; published online 4 April 2007)

Competitive binding between counterions around DNA molecule is characterized using the preferential interaction coefficient of individual ion in single and mixed electrolyte solutions. The canonical Monte Carlo (MC) simulation, nonlinear Poisson-Boltzmann (PB) equation, and density functional theory (DFT) proposed in our previous work [Wang, Yu, Gao, and Luo, J. Chem. Phys. **123**, 234904 (2005)] are utilized to calculate the preferential interaction coefficients. The MC simulations and theoretical results show that for single electrolyte around DNA, the preferential interaction coefficient of electrolyte decreases as the cation size is increased, indicating that the larger cation has less accumulation ability in the vicinity of DNA. For the mixed electrolyte solution, it is found that cation diameter has a significant effect on the competitive ability while anion diameter has a negligible effect. It proves that the preferential interaction coefficients of all ions decrease as the total ionic concentration is increased. The DFT generally has better performance than the PB equation does when compared to the MC simulation data. The DFT behaves quite well for the real ionic solutions such as the $KCl-NaCl-H_2O$, $NaCl-CaCl_2-H_2O$, and $CaCl_2-MgCl_2-H_2O$ systems. © *2007 American Institute of Physics*.
[DOI: 10.1063/1.2713105]

I. INTRODUCTION

Investigation on ionic atmosphere of DNA and RNA in an electrolyte solution is highly motivated recently for the biological importance and typical polyelectrolyte features of nucleic acid. Thus a wide range of theoretical and experimental techniques have been utilized in this field. Since the Manning parameter ξ, defined as the ratio of the Bjerrum length to the axial charge spacing of DNA, is larger than unity, the electrolyte solution is electrostatically unstable.[1,2] To lower the energy of solution, counterions accumulate around DNA molecule and form electric double layer (EDL). Many experiments have proven that the conformation transition of DNA is strongly dependent on the electrolyte environment.[3,4] Theoretical studies also argue that the stability of aqueous DNA solution is governed by a balance between electrostatic and nonelectrostatic interaction (hard-core repulsion, etc.).

To quantify the contribution of ions to the stability of a polyelectrolyte in aqueous solution, it is fruitful to introduce the polyion-ion preferential interaction coefficient Γ,[5–7] which is defined as

$$\Gamma = \lim_{m_u \to 0} \left(\frac{m - m'}{m_u} \right), \tag{1}$$

where m' is the molar concentration of the electrolyte in the compartment where polyelectrolyte is absent, m is the molar concentration of the salt in the compartment that contains the polyelectrolyte, and m_u is the concentration of the polyion in units of molarity. The preferential interaction coefficient is an important thermodynamic property for it characterizes not only the exclusion of coions and accumulations of counterions around a polyion but also the nonideality of the solution due to the interactions between a polyelectrolyte and an electrolyte solution. It should be noted that the preferential interaction coefficient is measurable by experimental methods though the experimental data are only a few.

The dialysis equilibrium method[8] is a classical method to obtain the preferential interaction coefficient. The nuclear magnetic resonance have also been used to reveal thermodynamic properties of DNA electrolyte solution and the competitive binding of different species of cations.[9] Although new techniques such as x-ray diffraction[10] and small-angle neutron scattering[11] make it possible to observe the microscopic structure of EDL around DNA, it still has some problems in interpreting the results of such experiments. The more simulation and theoretical investigation are required for understanding EDL from a microscopic point of view.

To model the EDL around DNA, various levels of physical model have been applied including charged cylinder model,[12–14] helical polyion model,[15,16] groove model[17] and all-atom model[18] of DNA, and primitive and nonprimitive models of electrolyte solution. Although the complicated models give some accurate descriptions of the structure of DNA,[19] the simple charged cylinder model combined with the primitive model of electrolyte solution involves both electrostatic and nonelectrostatic interactions and thus catch

[a]Author to whom correspondence should be addressed. Electronic mail: yangxyu@mail.tsinghua.edu.cn

the basic characteristic properties of the EDL around DNA. Therefore we adopt this kind of model in this work.

In the past two decades, many simulation studies including canonical Monte Carlo (CMC) simulation,[13,14,17,18,20] grand canonical Monte Carlo (GCMC) simulation,[12,15,16] and molecular dynamics (MD) simulation[21] have been carried out. Although there are some molecular simulations with high accuracy, they are somewhat time consuming and are unsuitable to some conditions, such as very dilute electrolyte solution or the situation where solvent should be considered. While theoretical methods give an inexpensive and time-saving alternative in this field, the well-known Manning's[1,22] theory provides a convenient predictive framework of ion distributions based on the counterion condensation phenomenon. In spite of its oversimplification of physical models, it has a good consistency with some experimental results[4] and has recently been extended to elaborate a model of DNA.[23] Another classical theory known as Poisson-Boltzmann (PB) equation[24] has been applied to more complicated physical models such as all-atom model of DNA,[25] etc. As the classical PB theory neglects the excluded volume effect of small ions, it is not adequate for high bulk concentration or involving multivalent cation.[26] Whereas, many recent investigations modified the PB equation by including the effect of finite size of small ions.[27] Integral equation theory (IET) is another rigorous statistical mechanical theory for inhomogeneous fluid. Incorporating the effect of finite size of ions, IET has better performance in the electrolyte solution of high bulk concentration or multivalent cation presented than the PB theory does.[28] Unlike all the theories mentioned above, the density functional theory (DFT) is established based on the thermodynamic principle that the grand canonical potential has a minimum value when the system reaches its equilibrium.[29] Recently, a modified fundamental measure theory (MFMT) proposed by Yu *et al.*[28,30] in the framework of Rosenfeld's fundamental measure theory[31] (FMT) gives a very accurate evaluation of hard-sphere contribution. It makes DFT a promising theory in field of inhomogeneous fluid. The evaluation of electrical interaction is another difficulty in DFT, which is usually implemented by a quadratic Taylor expansion with respect to a uniform bulk fluid.[28,32,33] Gillespie *et al.*[34] developed a reference functional density, where the reference fluid is not the corresponding bulk solution but an inhomogeneous fluid.[35]

The preferential interaction coefficient is originally designed for the solution containing only one species of polyelectrolyte and one pair of cation and anion.[5] Recently, Ni *et al.*[6] extended this original definition to mixed cation system and use the PB equation and MC simulation to calculate the designated preferential interaction coefficients for the systems containing both divalent and monovalent cations. A similar work has been done by Patra and Yethiraj[36] for the equal ionic size system. Different from the work of Ni *et al.*[6] and Patra and Yethiraj[32,36] which are limited to the electrolyte solution with ions of equal diameters, we use the preferential interaction coefficient to quantify the competitive binding between the cations with different valence and size. In the present work, the DFT, PB equation, and MC simulations are utilized to obtain the preferential interaction coefficients of each ion in the mixed-size electrolyte solution. The version adopted in the present DFT study is the one developed in our previous work. The hard-sphere contribution to total excess free energy functional is evaluated using the MFMT and the electrical interaction term is obtained using a quadratic Taylor expansion with respect to a uniform fluid. The established DFT is adequate to investigate the DNA aqueous solution containing mixed-size ions. Then a nonlinear PB calculation and canonical MC simulations with self-consistent Coulombic correction are implemented under the same physical model.

The rest of this paper is organized as follow. In Sec. II we describe the molecular models of interested systems and details of MC simulation and DFT. Numerical results are given in Sec. III. Some conclusions are summarized in Sec. IV.

II. MODEL AND THEORY

A. Molecular model

According to the definition of preferential interaction coefficient, all of our studies focus on the infinitely dilute DNA solution. The systems containing an isolated DNA molecule with one species of anion and one or two species of cation are considered in this paper. The DNA molecule is modeled as an infinitely long, impenetrable, and uniformly charged cylinder. Corresponding to B-form DNA, the radius of the hard cylindrical core of the DNA is $R=0.8$ nm, and the charge spacing is $b=0.17$ nm. Ions surrounding DNA are modeled as charged hard spheres with various diameters σ_α. The solvent water is modeled as a continuous structureless media with invariant dielectric constant $\varepsilon=78.4$ at any position, corresponding to that of the pure water at $T=298$ K. All the radii and diameters involved in this paper indicate hydrated ones. The temperature of solution is $T=298$ K. Above models are the same as those in our previous work.[37]

B. Density functional theory

In grand canonical ensemble, the system reaches equilibrium when the grand canonical potential Ω is at its minimum value $\tilde{\Omega}$. By virtue of variational principle, the equilibrium distribution of ion i, $\{\tilde{\rho}_i\}$, is obtained from Euler equation,

$$\left.\frac{\delta\Omega[\{\rho_i\}]}{\delta\rho_i(r)}\right|_{\tilde{\rho}}=0, \quad \Omega[\{\rho_i\}]_{\tilde{\rho}}=\tilde{\Omega}. \tag{2}$$

The grand potential functional Ω for the system described in this paper can be expressed as a functional of ion density profiles through the Legendre transform,

$$\Omega[\{\rho_i\}]=F[\{\rho_i\}]+\sum_{i=1}^{N}\int d\mathbf{r}[V_i^{\mathrm{ext}}(\mathbf{r})-\mu_i]\rho_i(\mathbf{r}), \tag{3}$$

where $V_i^{\mathrm{ext}}(\mathbf{r})$ is the external field due to the DNA molecule, N is the total number of ionic species, μ_i is the chemical potential of ion i, and $F[\{\rho_i\}]$ represents the Helmholtz energy functional.

The Helmholtz energy functional should be expressed in a proper form. In general, it can be decomposed into four parts according to different types of interactions,

$$F[\{\rho_i\}] = F^{\mathrm{id}}[\{\rho_i\}] + F_{\mathrm{C}}^{\mathrm{ex}}[\{\rho_i\}] + F_{\mathrm{hs}}^{\mathrm{ex}}[\{\rho_i\}] + F_{\mathrm{el}}^{\mathrm{ex}}[\{\rho_i\}], \quad (4)$$

where the first term on the right of Eq. (4) is the ideal-gas contribution, which can be accurately obtained from classical statistical mechanics. The second term is the direct Coulomb contribution calculated by summing the electrostatic potential over the space. The third term denotes the hard-sphere contribution, which is calculated via the MFMT.[30,37] The last term of Eq. (4) is the electrostatic interaction, obtained through a second-order functional Taylor expansion of the residual Helmholtz free energy around a uniform fluid.[30,37] The expressions of direct correlation functions required by Taylor expansion method is usually obtained from mean spherical approximation.[37,38] Finally, electroneutrality condition should be imposed on Eqs. (2)–(4) to maintain the electroneutrality of the solutions.[37]

If the hard-sphere contribution is not involved in DFT, namely, the terms of $F_{\mathrm{hs}}^{\mathrm{ex}}[\{\rho_i\}]$ and $F_{\mathrm{el}}^{\mathrm{ex}}[\{\rho_i\}]$ are not included in Eq. (4), the DFT theory reduces to the classical nonlinear PB equation.

C. Canonical Monte Carlo simulation

We also use MC simulation method similar to our previous work.[37] Without any assumption and simplification, the MC method strictly follows the above physical models. The CMC simulations are carried out using a cylindrical simulation box with its axis coinciding with the axis of DNA molecule. A hard-wall outer boundary and a periodical boundary are imposed on the radial direction and axial direction of simulation box, respectively. The long-range energy of Coulomb is corrected by self-consistent method.[13]

The simulation starts by randomly placing the mobile ions within the simulation box but avoiding overlap. The external potential is obtained from the ion distributions of central cell according to self-consistent algorithm[13,39] and renewed for appropriate interval. After approximately 7.0×10^7 pre-equilibrium MC steps, the equilibrium of the system is achieved. Then five consecutive blocks, each has 5.0×10^7 steps, are performed to obtain the preferential interaction coefficients and their uncertainties.[14] Because of the huge number of MC steps used here, the relative uncertainties of results are very small ($<0.1\%$) that are even unable to be plotted in the figures. Since bulk concentrations of ions cannot be obtained from the CMC simulation directly, a large enough simulation box gets the bulk concentrations in the middle position between DNA surface and the outer boundary of the simulation box in radial direction. To obtain the desired bulk ionic concentrations, trial-and-error method is used in pre-equilibrium process by changing the ion numbers and moving outer boundary successively. The difference between bulk ionic concentrations from simulation and the desired concentrations has proved to be negligible (relative error $<0.5\%$).[37]

III. RESULTS AND DISCUSSION

As mentioned in Sec. I, the preferential interaction coefficient can be used as a measurement of the accumulation of counterions and the repulsion of coions, as well as a measurement of nonideality of polyelectrolyte solution. We now concern polyelectrolyte solutions with more than one species of cations. As is verified in the following of this paper, the preferential interaction coefficient can be used as a criterion to quantify the ability of competitive binding between counterion species, especially for cation species with the same valence. When using theoretical methods, the preferential interaction coefficient for each species i is calculated by numerical integration of ion distributions,[33]

$$\Gamma_i = 2\pi b \int_0^\infty dr r[\rho_i(r) - \rho_i^b], \quad (5)$$

where, subscript i indicates that the variable is for ion species i and the superscript b means that the variable is for the bulk, r is the radial distance between the ion center and the DNA axis. For MC simulation, the ion distributions are unnecessary. The preferential interaction coefficient is obtained from configurations after equilibration,

$$\Gamma_i = \{N_i\}_{R_c} - \{N_i^{\mathrm{bulk}}\}_{R_c}, \quad (6)$$

where the $\{\}$ means average over configurations; subscript R_c means statistics are carried out within R_c, which should be set large enough to get bulk concentration at $r=R_c$; N_i denotes total ion number within $r=R_c$; and N_i^{bulk} denotes the number of ions i located within R_c with bulk concentration. In the present study, the Picard iteration method is used in DFT calculation and the ratio of time consumed by MC simulation and DFT computation is about 10:1. The computational time of DFT can be reduced greatly if an optimized algorithm is employed.

A. Effect of cation sizes on the competitive ability

Figure 1 shows the cation size influence on preferential interaction coefficient predicted by the MC simulation, DFT, and PB equation for the systems containing model DNA molecule and a single 1:1 electrolyte. The bulk concentration of the counterion and coion is fixed at 0.3 mol/l, while diameter of cation varies from 0.1 to 0.6 nm. It is found that the preferential interaction coefficient of salt declines as cation size is increased. It indicates that the larger cation has less accumulation ability in the vicinity of DNA. This phenomenon mainly attributes to the volume exclusion of ions and DNA, namely, the same volume around DNA intends to accommodate fewer ions when cation becomes larger. The curves predicted by DFT are more accurate than those from the PB equation with respect to MC results. Without any mechanism to include volume exclusion effect, the only parameter which considers the ion size in the PB equation is the minimal separation between ionic center and DNA surface, i.e., $\sigma_\alpha/2$. Figure 2 displays the cation size influence on preferential interaction coefficient of a single 2:1 electrolyte around DNA. The bulk concentration of the electrolyte is fixed at 0.2 mol/l. The same conclusions can be drawn from

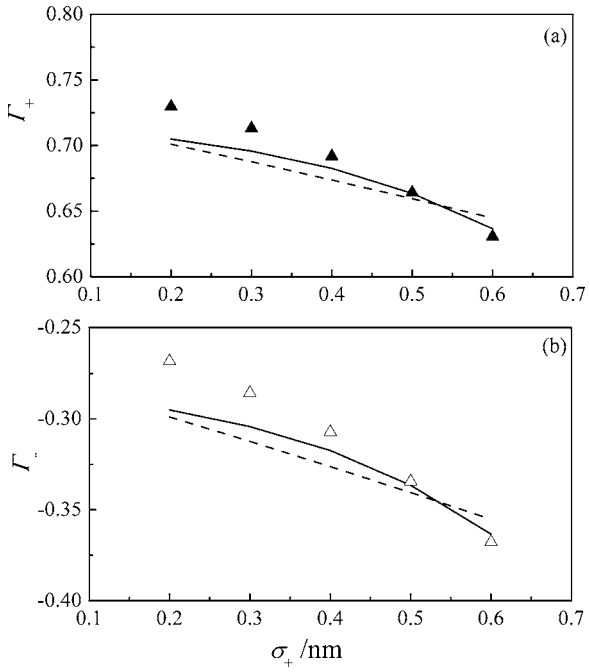

FIG. 1. Preferential interaction coefficient of (a) cation and (b) anion as a function of cation size for 1:1 electrolyte around DNA. The bulk concentration of electrolyte is fixed at 0.3 mol/l and the anion diameter is fixed at 0.4 nm. The points, dashed, and solid lines represent the results from the MC simulation, PB equation, and DFT, respectively.

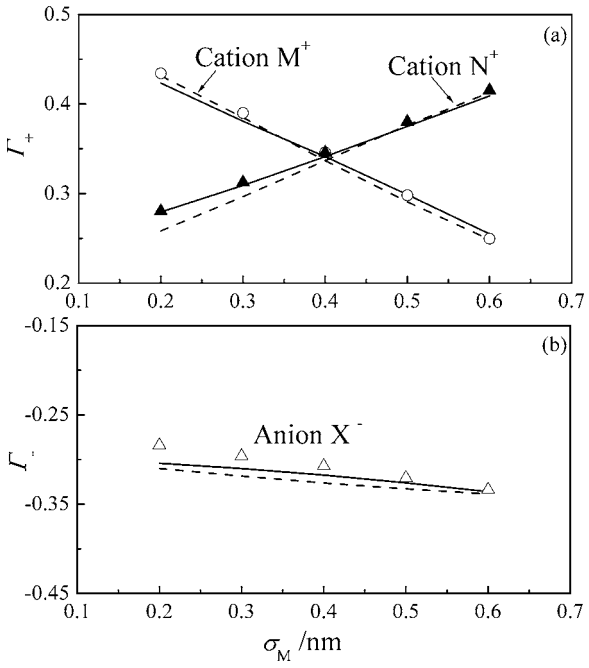

FIG. 3. Preferential interaction coefficients of (a) cation and (b) anion as functions of cation diameter for the $MX-NX-H_2O$ system. The diameters of both cation N^+ and anion X^- are fixed at 0.4 nm, and the bulk concentrations of both cation M^+ and N^+ are 0.150 mol/l. The symbols, dashed, and solid lines represent the MC, PB, and DFT results, respectively.

this figure. Although the results of DFT for the single 2:1 electrolyte solution are not so good as those for the single 1:1 electrolyte, we can see that the results from the DFT become more accurate as the cation size is increased. It should be noticed that in the case of small cation the DFT results are close to those of the PB results, while in the case of larger cation the DFT results are more close to MC results. This is because when cation is small the long-range Coulombic interactions between the ion-ion and ion-polyion are dominant, and otherwise the excluded volume effect is dominant. Therefore, it can be concluded from Figs. 1 and 2 that for single electrolyte (both 1:1 and 2:1) solutions, the preferential interaction coefficients for both cation and anion are decreased as the cation diameter is increased. However, the effect of anion size on the preferential interaction coefficient is only marginal.

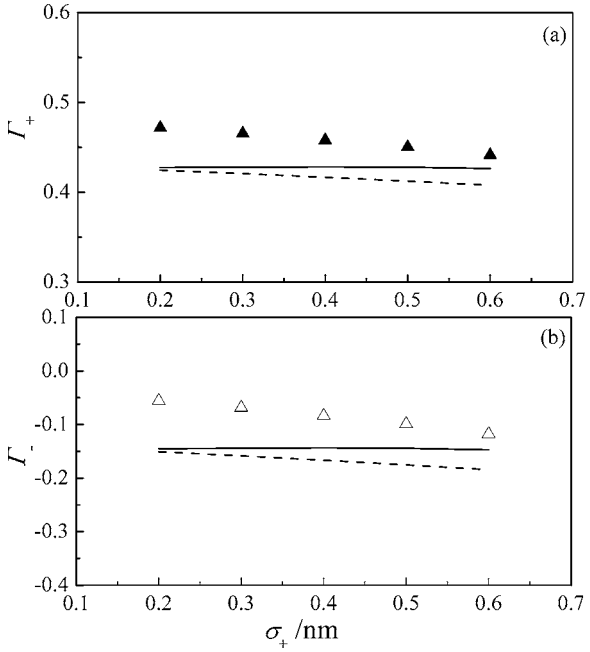

FIG. 2. Preferential interaction coefficient of (a) cation and (b) anion as a function of cation size for 2:1 (MX_2) electrolyte around DNA. The bulk concentration of electrolyte is fixed at 0.2 mol/l and the anion diameter is fixed at 0.4 nm. The meanings of the symbols and curves are the same as in Fig. 1.

Figures 3 and 4 depict the dependence of preferential interaction coefficient on diameter of cation 1 (M^+ or M^{2+}) for the $MX-NX-H_2O$ and $MX_2-NX_2-H_2O$ systems, respectively. Figure 3 indicates the case that two monovalent cations competitively accumulate around the DNA, and Fig. 4 is that for divalent cations. In both Figs. 3 and 4 the two competitive cations have the same diameters. The diameters of cation 2 (N^+ or N^{2+}) and anion as well as total cation bulk concentration are fixed, while diameter of cation 1 (M^+ or M^{2+}) varies from 0.1 to 0.6 nm. All the three methods predict most linear variation of preferential interaction coefficients with the increase of cation 1 diameter. Figures 3(a) and 4(a) show that as the size of one cation is increased the preferential interaction of anion only slightly declines. This is because of the excluded volume effect as discussed in the above paragraph. According to the definition of preferential interaction coefficient,[6] we obtain $\Sigma_i z_i \Gamma_i = 1$ therefore the total preferential interaction coefficient of cations equals $(1-\Gamma_a)/z_c$, where Γ_a denotes the preferential interaction coefficient of anion and z_c denotes the valence of cations. Compared with those of anion, the preferential interaction coefficient of individual cation species varies more intensively

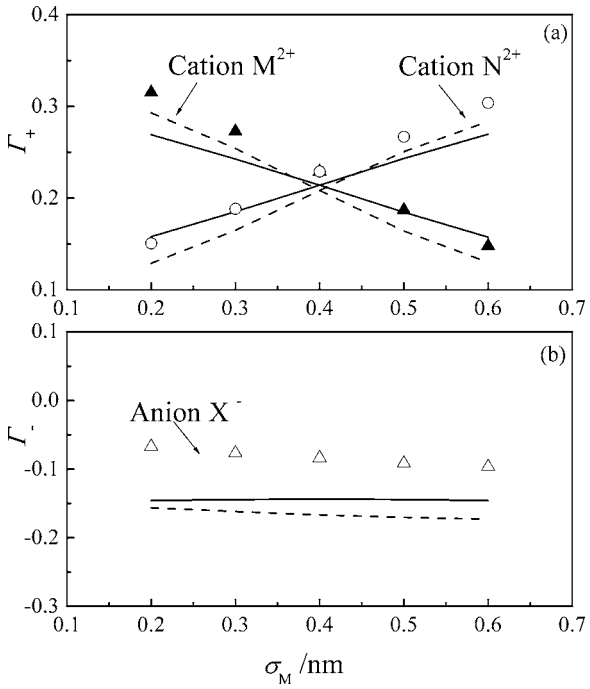

FIG. 4. Preferential interaction coefficients of (a) cation and (b) anion as functions of cation diameter for the $MX_2-NX_2-H_2O$ system. The diameters of both cation N^{2+} and anion X^- are fixed at 0.4 nm, and the bulk concentrations of both cation M^{2+} and N^{2+} are 0.050 mol/l. The meanings of the symbols and lines are the same as in Fig. 3.

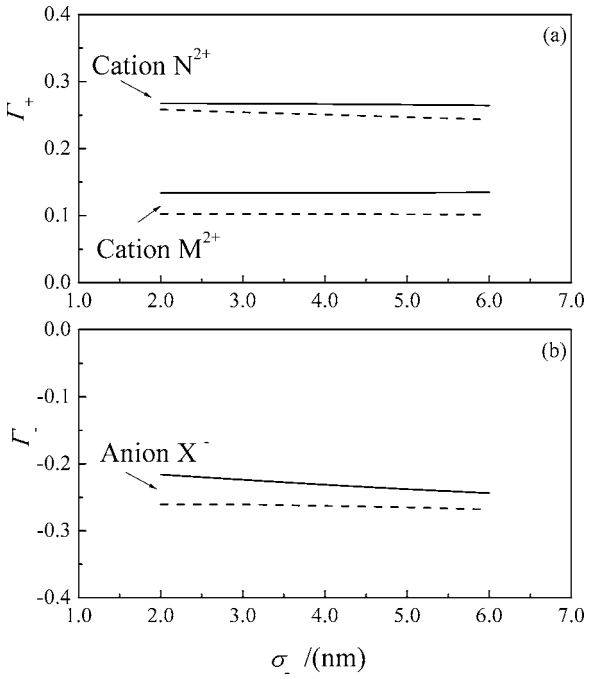

FIG. 5. Preferential interaction coefficients of (a) cation and (b) anion as functions of anion diameter for the $MX_2-NX_2-H_2O$ system. The diameters of cation N^{2+} and cation M^{2+} are fixed at 0.6 and 0.4 nm, respectively. The bulk concentrations of cation N^{2+} and cation M^{2+} are both 0.050 mol/l. The meanings of the symbols and lines are the same as in Fig. 3.

than those of the total ones. It proves the existence of the competition between two cations. As the diameter of cation 1 becomes small, its competitive ability improves. Then cation 1 accumulates more around DNA and pushes more ion of cation 2 away from the surface of DNA. From Figs. 3(b) and 4(b), it is found that the preferential interaction coefficients of anion and total cations predicted from the DFT are better than that from the PB equation when compared to the MC results. However, for the preferential interaction coefficient of each cation the DFT is not always better than the PB equation. The DFT gives better prediction for the larger cation, showing that the accuracy of the DFT depends on the proportion of hard-sphere contribution to Helmholtz free energy. If one cation is relatively larger than another, the hard-sphere contribution to Helmholtz free energy is greater than that of the smaller one, and thus the DFT gives excellent prediction of this cation. The influence of anion diameter on the preferential interaction coefficient is predicted from the PB equation and DFT, and the results are plotted in Fig. 5. As displayed in this figure, anion diameter has negligible effect on both anion and cation preferential interaction coefficient due to the extremely low density of anion in the vicinity of DNA.

B. Effect of bulk concentration on competitive ability

Figure 6 reveals the dependence of preferential interaction coefficient on the bulk concentration ratio between two monovalent cations for the $MX-NX-H_2O$ system. Figure 6(a) shows that the competition between two cations with the same valence is not only affected by the ion size but also controlled by the ratio of bulk concentration. The preferential interaction coefficient of cation M^+ increases as the bulk concentration ratio C_M^b/C_N^b is increased, where C_M^b and C_N^b represent the bulk molar concentrations of M^+ and N^+, respectively. The preferential interaction coefficient of anion

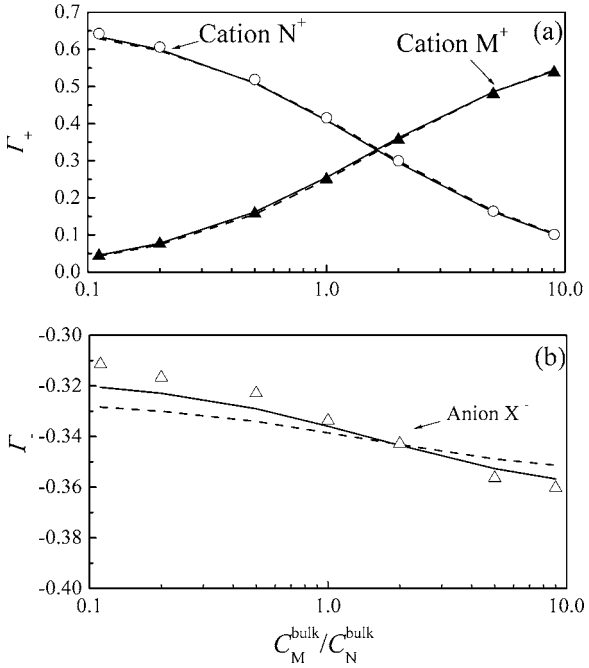

FIG. 6. Preferential interaction coefficients of (a) cation and (b) anion as functions of the bulk concentration ratio between two cations for the $MX-NX-H_2O$ system. The diameters of cation M^+, cation N^+, and anion X^- are 0.6, 0.4, and 0.4 nm, respectively, and the total concentration of cations is fixed at 0.3 mol/l. The meanings of the symbols and lines are the same as in Fig. 3.

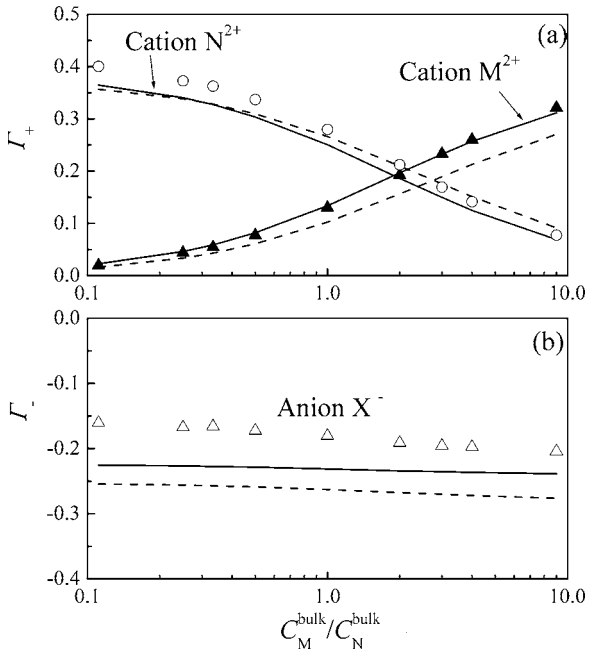

FIG. 7. Preferential interaction coefficients of (a) cation and (b) anion as functions of the bulk concentration ratio between two divalent cations for the $MX_2-NX_2-H_2O$ system. The diameters of cation M^{2+}, N^{2+}, and anion X^- are 0.6, 0.4, and 0.4 nm, respectively, and the total concentration of cations is fixed at 0.2 mol/l. The meanings of the symbols and lines are the same as in Fig. 3.

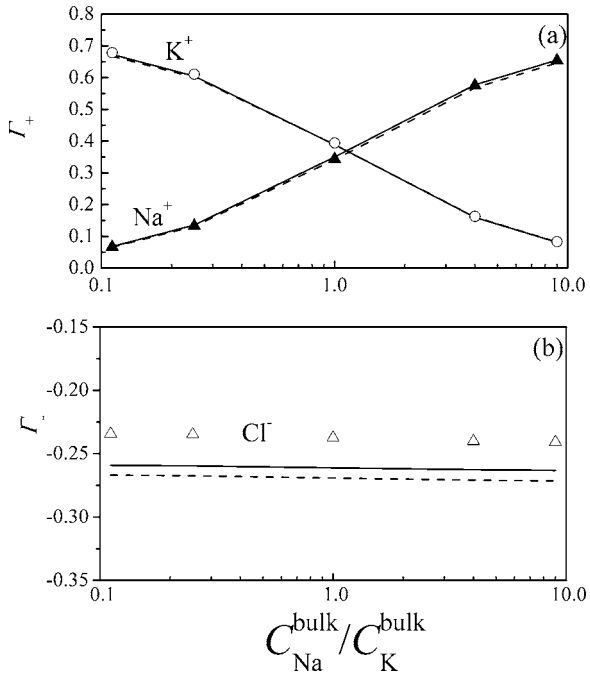

FIG. 8. Preferential interaction coefficients of (a) cation and (b) anion as functions of the bulk concentration ratio between two cations for the $KCl-NaCl-H_2O$ system. The diameters of K^+, Na^+, and Cl^- are 0.324, 0.376, and 0.4 nm, respectively, and the total concentration of cations is fixed at 0.2 mol/l. The meanings of the symbols and lines are the same as in Fig. 3.

has a slight decline as the concentration ratio C_M^b/C_N^b is increased, due to the volume exclusion effect. These conclusions are also true for the divalent cation as shown in Fig. 7. For the monovalent cation system, both the DFT and PB equation make an excellent prediction for preferential interaction coefficients of cations, while the DFT predicts better results for anion than that of the PB equation. From Fig. 7 one can see that for the divalent cation system the DFT is also superior to the PB equation, except the prediction for smaller cation. The systems of $KCl-NaCl-H_2O$ and $CaCl_2-MgCl_2-H_2O$ are also investigated and the results are plotted in Figs. 8 and 9, respectively. A natural consequence of the dielectric continuum approximation is the introduction of "effective" radii of small ions. The effective diameters of Na^+, K^+, Ca^{2+}, Mg^{2+}, and Cl^- used in this work are taken from Korolev *et al.*[16] because they reproduce good experimental data for the bulk electrolyte solutions. The preferential interaction coefficients predicted by DFT using real ion diameters are in good consistency with MC result for either cation species or anion in both situations of monovalent and divalent cations. The reason why DFT gives good predictions for all divalent cation is that the real divalent cation, even the smallest one, has enough large size to obtain good accuracy. In other words, the DFT is adequate to predict the ion competition for real electrolyte around DNA.

There exists a crossover point of the curves for the preferential interaction coefficients of the two cations in Figs. 6–9. At these points the accumulations of the two cations in the vicinity of DNA are equal. The equivalency is based on the balance of the effect of ion size and bulk concentration. In Figs. 6(a), 7(a), 8(a), and 9(a), the bulk concentration ratio between two cations at crossover points takes account of the influence of both bulk concentration ratio and ion size and may be used to characterize the relative competitive ability of the two competitive counterions.

The influence of equivalent fraction of monovalent cat-

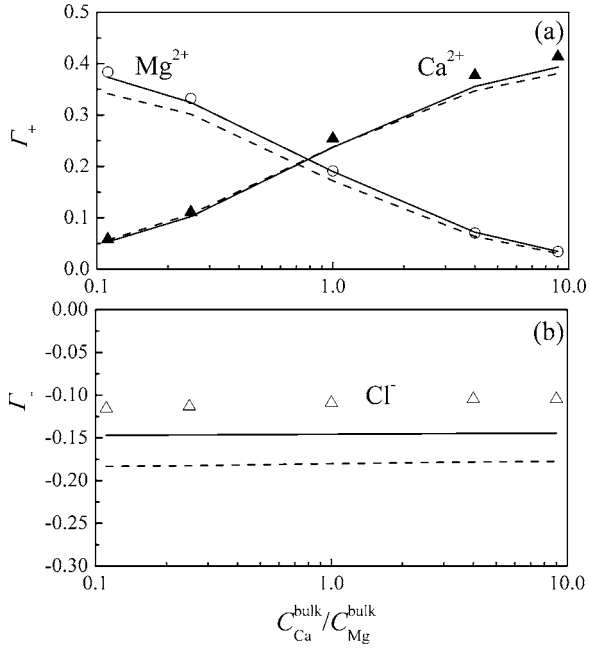

FIG. 9. Preferential interaction coefficients of (a) cation and (b) anion as functions of the bulk concentration ratio of two divalent cations for the $MgCl_2-CaCl_2-H_2O$ system. The diameters of Ca^{2+}, Mg^{2+}, and Cl^- are 0.52, 0.6, and 0.4 nm, respectively, and the total concentration of cations is fixed at 0.2 mol/l. The meanings of the symbols and lines are the same as in Fig. 3.

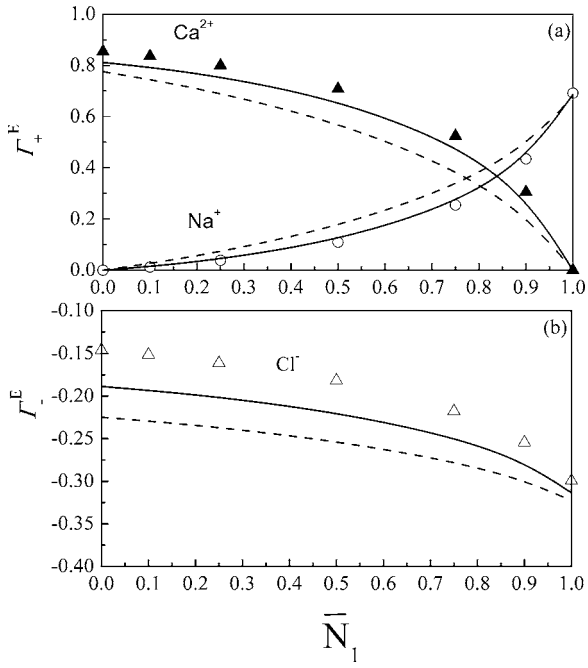

FIG. 10. Equivalent preferential interaction coefficients of (a) cation and (b) anion as functions of the equivalent fraction of monovalent cation for the $NaCl-CaCl_2-H_2O$ system. The diameters of Ca^{2+}, Na^+, and Cl^- are 0.52, 0.376, and 0.4 nm, respectively and the total concentration of anions is fixed at 0.3 mol/l. The meanings of the symbols and lines are the same as in Fig. 3.

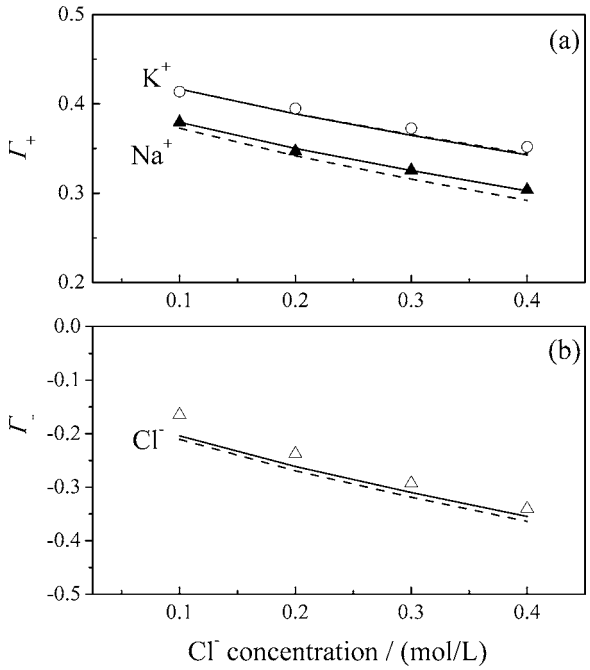

FIG. 11. Preferential interaction coefficients of (a) cation and (b) anion as functions of the anion concentration for the $KCl-NaCl-H_2O$ system. The diameters of K^+, Na^+, and Cl^- are 0.324, 0.376, and 0.4 nm, respectively, and bulk concentration ratio between two cations is fixed at 1:1. The meanings of the symbols and lines are the same as in Fig. 3.

ion $\bar{N}_1$ on the equivalent preferential interaction coefficients for the $NaCl-CaCl_2-H_2O$ system is shown in Fig. 10. The equivalent fraction of monovalent cation is expressed by

$$\bar{N}_1 = \frac{|z_1|\rho_1^b}{|z_2|\rho_2^b + |z_1|\rho_1^b}$$

where ρ_1^b denotes the bulk concentration of monovalent cation, and ρ_i^b and z_i $(i=1,2)$ denote the bulk concentration and valency of the cation i. Here, we use equivalent preferential interaction coefficients Γ_i^E, expressed as $|z_i|\Gamma_i$, to compare the preferential interaction coefficients between the cations with different valencies. The multivalent cation can be regarded as binding a few monovalent cations together. However, the volume of it is about 2.6 times as large as that of Na^+, while competitive ability of Ca^{2+} proves to be much stronger than that of Na^+ in Fig. 10. It indicates that the effect of valency on competitive ability is much greater than that of volume.

Figures 11 and 12 depict the dependence of preferential interaction coefficient on the total bulk concentration for the $KCl-NaCl-H_2O$ and $CaCl_2-MgCl_2-H_2O$ systems, respectively. In both figures, the bulk concentrations of the two cations are the same. The preferential interaction coefficients of both two competitive counterions decrease as the total bulk concentration of cations is increased. The DFT generally gives better results than the PB equation does, especially for the larger cations. The PB equation always underestimates the preferential interactions coefficients of all ions for both $KCl-NaCl-H_2O$ and $CaCl_2-MgCl_2-H_2O$ systems.

IV. CONCLUDING REMARKS

Competitive binding of two cations with the same valence to DNA molecule in aqueous solution is investigated using the Monte Carlo (MC) simulation, density functional theory (DFT), and Poisson-Boltzmann (PB) equation. In the

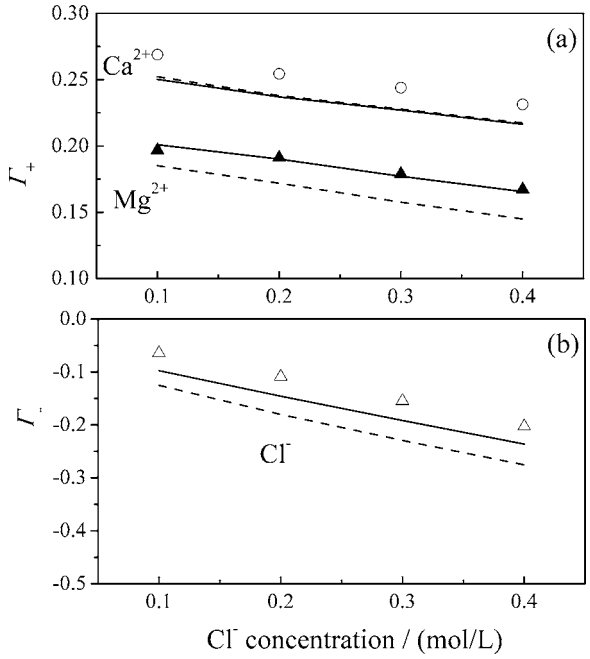

FIG. 12. Preferential interaction coefficients of (a) cation and (b) anion as functions of the anion concentration for the $CaCl_2-MgCl_2-H_2O$ system. The diameters of Ca^{2+}, Mg^{2+}, and Cl^- are 0.52, 0.6, and 0.4 nm, respectively, and the bulk concentration ratio between two cations is fixed at 1:1. The meanings of the symbols and lines are the same as in Fig. 3.

present DFT, the modified fundamental measure theory proposed by Yu *et al.*[28,30] is used to evaluate the hard-sphere contribution to the free energy functional, and the electrical interaction is obtained through a quadratic Taylor expansion around a corresponding uniform fluid. In the MC simulations, an iterative self-consistent method[13,39] is proposed to correct the long-range Coulombic energy.

The preferential interaction coefficient of each cation is used to measure the competitive ability of this cation around DNA in single and mixed electrolyte solutions. The effects of ion size and bulk concentration on preferential interaction coefficients are investigated extensively. The cation diameter is proved to be a significant parameter in competitive ability. The smaller cation has stronger competitive ability than the larger one in the system of interest. It is also found that anion diameter has a negligible effect on preferential interaction coefficient of either cation or anion. The bulk concentration ratio also makes strong impact on competitive ability of cations. The concentrated cation always has superiority in competition to the relative dilute one. To integrate the effect of both ion size and bulk concentration ratio, the bulk concentration ratio at the crossover point where the preferential interaction coefficients of two competitive cations are equal can be used to characterize the relative competitive ability of certain cation species. It is a relative stable point with respect to the change of total cation concentration. It is also found that the preferential interaction coefficient of all ions decreases as the total cation concentration is increased.

The calculations involved in this work suggest that the results from the DFT generally are better than those from the PB equation when compared to the corresponding MC results. The present DFT evaluates the hard-sphere contribution to Helmholtz free energy accurately due to the good performance of the MFMT, and the evaluation of electrostatic interaction is simply implemented by quadratic Taylor expansion with respect to a uniform fluid. Therefore, the present DFT is applicable to the system where the hard-sphere contribution takes more proportion in Helmholtz free energy, such as monovalent cation solution, or large divalent cation solution. Fortunately, the DFT has good performance for all cations in the real systems studied in this work since the real divalent cations like Mg^{2+} and Ca^{2+} have an enough large diameter.

ACKNOWLEDGMENT

The authors gratefully acknowledge the financial support from the National Natural Science Foundation of China under Project Grant Nos. 20376037 and 20490200.

[1] G. S. Manning, Q. Rev. Biophys. **11**, 179 (1978).
[2] G. S. Manning, Physica A **11**, 179 (1996).
[3] R. V. Gessner, G. J. Quigley, A. H. J. Wang, G. A. van der Maarel, J. H. V. Boom, and A. Rich, Biochemistry **24**, 237 (1985); T. M. Record, Annu. Rev. Biochem. **50**, 997 (1981).
[4] C. F. Anderson and T. M. Record, Annu. Rev. Phys. Chem. **33**, 191 (1982).
[5] H. Eisenberg, *Biological Macromolecules and Polyelectrolytes in Solution* (Oxford, Clarendon, 1976).
[6] H. Ni, C. F. Anderson, and T. M. Record, Jr., J. Phys. Chem. B **103**, 3489 (1999).
[7] K. A. Sharp, Biopolymers **36**, 227 (1995); C. H. Taubes, U. Mohanty, and S. Chu, J. Phys. Chem. B **109**, 21267 (2005).
[8] J. Shack, R. J. Jenkins, and J. M. Thompsett, J. Biol. Chem. **198**, 85 (1952); U. P. Strauss, C. Helfgott, and H. Pink, J. Phys. Chem. **71**, 2550 (1967).
[9] H. S. Harned and B. B. Owen, *The Physical Chemistry of Electrolyte Solution* (Reinhold, New York, 1958); R. L. Kay, in *Water: A comprehensive Treatise* edited by F. Franks (Plenum, New York, 1973).
[10] R. Das, T. T. Mills, L. W. Kwok, G. S. Maskel, I. S. Millett, S. Doniach, K. D. Finkelstein, D. Herschlag, and L. Pollack, Phys. Rev. Lett. **90**, 188103 (2003).
[11] S. S. Zakharova, S. U. Eqelhaaf, L. B. Bhuiyan, C. W. Outhwhaite, D. Bratko, and J. R. C. van der Maarel, J. Chem. Phys. **111**, 10706 (1999).
[12] V. Vlachy and D. J. Haymet, J. Chem. Phys. **84**, 5874 (1986).
[13] P. Mills, C. F. Anderson, and M. T. Record, Jr., J. Phys. Chem. **89**, 3984 (1985).
[14] H. Ni, C. F. Anderson, and T. M. Record, Jr., J. Phys. Chem. B **103**, 3489 (1999).
[15] N. Korolev, A. P. Lyubartsev, A. Rupprecht, and L. Nordenskiold, J. Phys. Chem. B **103**, 9008 (1999).
[16] N. Korolev, A. P. Lyubartsev, A. Rupprecht, and L. Nordenskiold, Biophys. J. **77**, 2736 (1999).
[17] J. C. G. Montoro and J. L. F. Abascal, J. Chem. Phys. **103**, 8273 (1995).
[18] G. R. Pack, L. Wong, and G. Lamm, Biopolymers **49**, 575 (1999).
[19] S. Y. Ponomarev, K. M. Thayer, and D. L. Beveridge, Proc. Natl. Acad. Sci. U.S.A. **101**, 14771 (2004); K. Anderson, R. Das, H. Y. Park, H. Smith, L. W. Kwok, J. S. Lamb, E. J. Kirkland, D. Herschlag, K. D. Finkelstein, and L. Pollack, Phys. Rev. Lett. **93**, 248103 (2004).
[20] M. Le Bret and B. H. Zimm, Biopolymers **23**, 271 (1984).
[21] M. Deserno, F. Jimenez-Angeles, C. Holm, and M. Lozada-Cassou, J. Phys. Chem. B **105**, 10983 (2001).
[22] G. S. Manning, Biophys. Chem. **7**, 95 (1977).
[23] F. Fogolari, P. Zuccato, G. Esposito, and P. Viglino, Biophys. J. **76**, 1 (1999).
[24] M. Gouy, J. Phys. **9**, 457 (1910); D. L. Chapman, Philos. Mag. **25**, 475 (1913).
[25] B. Jayaram and D. L. Beveridge, Annu. Rev. Phys. Chem. **25**, 367 (1996).
[26] M. Fixman, J. Chem. Phys. **70**, 4995 (1979); S. L. Carnie and G. M. Torrie, Adv. Chem. Phys. **56**, 141 (1984); L. Degreve and M. Lozada-Cassou, Mol. Phys. **86**, 759 (1995).
[27] C. W. Outhwhaite and L. B. Bhuiyan, Mol. Phys. **74**, 367 (1991); L. B. Bhuiyan and C. W. Outhwhaite, J. Chem. Phys. **116**, 2650 (2002); T. Das, D. Bratko, L. B. Bhuiyan, and C. W. Outhwhaite, *ibid.* **107**, 9197 (1997); L. B. Bhuiyan, C. W. Outhwaite, and D. Henderson, Langmuir **22**, 10630 (2006).
[28] Y.-X. Yu, J. Wu, and G.-H. Gao, J. Chem. Phys. **120**, 7223 (2004).
[29] M. Lozada-Cassou, in *Fundamentals of Inhomogeneous Fluids*, edited by D. Henderson (Marcel Dekker, New York, 1992).
[30] Y.-X. Yu and J. Wu, J. Chem. Phys. **117**, 10156 (2002).
[31] Y. Rosenfeld, Phys. Rev. Lett. **63**, 980 (1989); Y. Rosenfeld, J. Chem. Phys. **93**, 4305 (1990); Y. Rosenfeld, *ibid.* **98**, 8126 (1993).
[32] C. N. Patra and A. Yethiraj, J. Phys. Chem. B **103**, 6080 (1999).
[33] K. Wang, Y.-X. Yu, and G.-H. Gao, Phys. Rev. E **70**, 011912 (2004).
[34] D. Gillespie, W. Nonner, and R. S. Eisenberg, J. Phys.: Condens. Matter **14**, 12129 (2002); D. Gillespie, W. Nonner, and R. S. Eisenberg, Phys. Rev. E **68**, 031503 (2002).
[35] O. Pizio, A. Patrykiejew, and S. Sokolowski, J. Chem. Phys. **121**(23), 11957 (2004); J. Reszko-Zygmunt, S. Sokolowski, D. Henderson, and D. Boda, *ibid.* **122**, 084504 (2005).
[36] C. N. Patra and A. Yethiraj, Biophys. J. **78**, 699 (2000).
[37] K. Wang, Y.-X. Yu, G.-H. Gao, and G.-S. Luo, J. Chem. Phys. **123**, 234904 (2005).
[38] M. Valisko, D. Henderson, and D. Boda, J. Phys. Chem. B **108**, 16548 (2004); K. Hiroke, Mol. Phys. **33**, 1195 (1977).
[39] C. Murthy, R. J. Bacquet, and P. J. Rossky, J. Phys. Chem. **89**, 701 (1985).